

Free Convective Effects on Stokes Flow Mass Transfer

R. S. PEARSON and P. F. DICKSON

Colorado School of Mines, Golden, Colorado

Free convective effects on forced convective mass transfer in the Stokes flow region were studied experimentally by using a single drop in a liquid-liquid system.

Liquids used to form the drops were methyl acetate or 2-ethoxyethyl acetate with distilled water as the continuous medium. Spherical drops were formed on the capillary tip of a 0.58 cm. O.D. capillary glass tube centered in a 2.5 cm. O.D. pyrex tubular flow cell.

Results are presented graphically as N_{Sh} vs. N_{Pe} , N_{Sh} vs. N_{Re} , and $N_{Sh}/N_{Ra}^{1/4}$ vs. N_{Pe} to show the variation of mass transfer with flow rate and free convection. The range of variables was $10 \leq N_{Pe} \leq 35,000$; $0.1 \leq N_{Re} \leq 30$; $578 \leq N_{Sc} \leq 1,149$; and $12.3 \leq N_{Gr} \leq 75.7$.

Satisfactory comparisons were also made with other investigators' findings.

Results substantiate that at low flow rates (Reynolds number < 10 , Peclet number $< 1,000$) free convective effects either reinforce or interfere with mass transfer. This interference takes place until flow becomes high enough to overcome interfering effects of free convection.

Although many experimental and theoretical studies of mass and heat transfer have been conducted, few data are available on mass transfer in the Stokes flow region. In the limit of no flow (pure diffusion), one has the analytical result for mass transfer of $N_{Sh} = 2$. For Peclet number on the order of 1,000 and greater, a number of correlations are available. In real systems, free convection adds complications to the transfer picture.

The subject of heat and mass transfer from spherical and cylindrical shapes has been investigated in a variety of studies. Experimental data have been taken over a broad range of Reynolds numbers ($Re > 60$), producing results which have acceptable agreement with theoretical work in the region where forced convection predominates (1 to 13). In low Reynolds number regions, free convective effects cause deviation from predictions which consider forced convection alone. Theoretical results (8, 14, 15) show the parameter N_{Gr}/N_{Re}^2 to be of fundamental importance in the gradual transition from free to forced convective control, and the mechanisms of free and forced convection to be nonadditive.

Work by Garner and associates (6, 16, 21) on mass transfer from solid spheres of benzoic and adipic acid to water indicated that, at Reynolds number below four, the Sherwood number seemed to be the same as that for molecular diffusion and free convection. For free convection with Schmidt number greater than 100, these authors (6, 16) found, both theoretically and experimentally that $N_{Sh} \propto N_{Ra}^{1/4}$ for laminar conditions. A depression of Sherwood number between Reynolds numbers of 20 and 60 was also found with Rayleigh numbers greater than 10^6 . Explanation was a mass transfer hindrance or promotion of bulk flow by free convective effects.

Steinberger and Treybal (17) conducted an investigation concerning mass transfer from solid benzoic acid spheres to water for forced and free convection. Reynolds numbers ranged from 10 to 16,920; Schmidt numbers from

987 to 69,680; and Grashof numbers from 5,130 to 125,200. In free convection with Rayleigh number less than 10^8 , the authors (17) present

$$N_{Sh,o} = 2 + 0.569 (N_{Gr} N_{Sc})^{1/4}$$

with an average deviation for their data of 12.7%. For combined free and forced convection, their final correlation became:

$$N_{Sh} = N_{Sh,o} + 0.347 (N_{Re} N_{Sc}^{1/2})^{0.62}$$

This equation correlates their data and data from other literature very well over a range of $1 < (Re Sc^{1/2}) < 500,000$ for both mass and heat transfer, but with the notable exception of the data of Garner and Kee (16).

The present work is an experimental attempt to study the relationship between mass transfer and flow rate for the Stokes Flow region with free convective effects present.

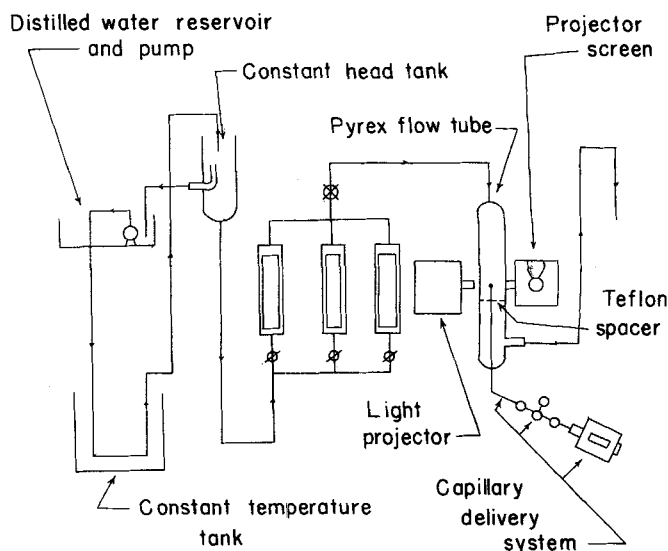


Fig. 1. Flow diagram of experimental apparatus.

R. S. Pearson is with Continental Oil Company, Ponca City, Oklahoma.

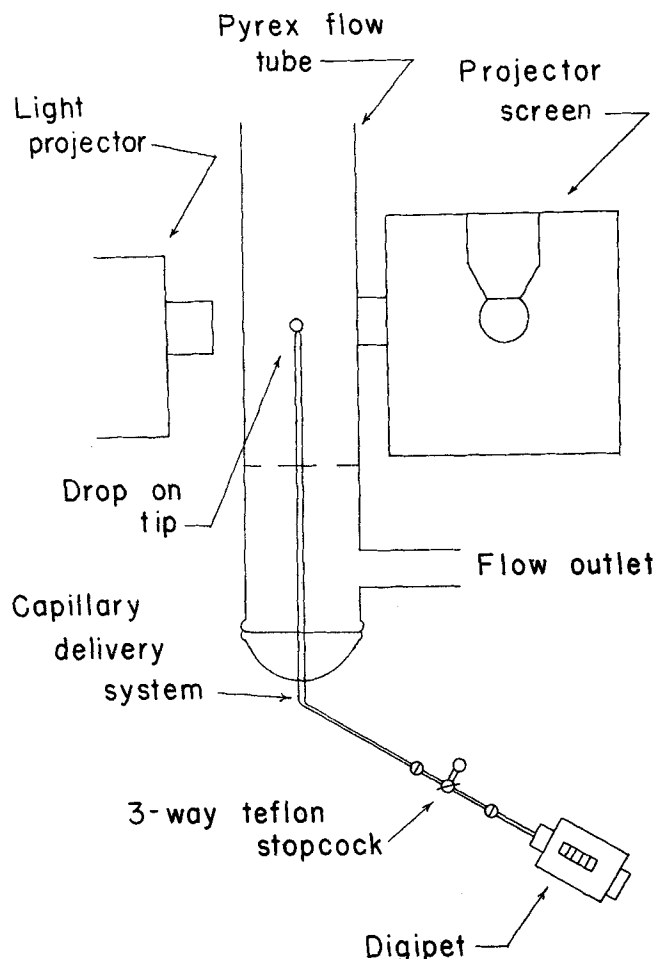


Fig. 2. Diagram of mass transfer system.

EXPERIMENTAL

Apparatus and Equipment

Experimental apparatus may be grouped as follows: diffusion chamber, distilled water delivery, and organic liquid delivery. A schematic is shown in Figure 1.

A pyrex tube of 2.5 cm. diam. and 16 in. length housed the basic transfer system and served as a channel for distilled water flow.

The organic phase delivery tube, a 0.58 cm. diam. glass capillary tube with a ground tip, was inserted along the axis of the pyrex tube from the water exit end. This tip was hand-ground to an angle of 60 degrees with end area of 0.0031 sq. cm. Attachment of the capillary to the cylinder was by means of a glass bell with an O-ring joint and clamp. To insure centering of the tip on the cylinder axis, teflon spacers were made of O. D. equal to cylinder I. D. and with a center hole for the capillary tube and numerous holes for water passage. Positioning of the diffusion cell was vertical with water flow either upward or downward. In operation, an organic drop on the end of the capillary diffused into the water stream flowing past it in the pyrex tube. A drawing of the diffusion cell is given in Figure 2.

Delivery of distilled water to the diffusion cell was from a tank with approximately 2 ft. of water head. Level in the constant head tank was maintained by circulation of water from a supply reservoir using a bronze immersion pump (No. 54901, VW and R) rated at 75 g./hr. capacity. To insure elimination of any pump heating effects, this flow was passed through 15 ft. of copper tubing immersed in a constant temperature bath. From the constant head tank, water was fed to one of a bank of three Fisher and Porter rotameters with an overall flow rate range of 0.001-1.5 cc./sec. Calibration of these rotameters was by timed volume of delivery. From a needle valve which controlled flow from the rotameter in use, water passed into the entrance of the diffusion chamber, past the diffusing organic drop and from the chamber. Exit of this fluid was passed to a height equal to that of the needle valve to eliminate a suction on both rotameter float and diffusing drop.

The fluid then dropped freely in a large diameter glass tube to be either collected or discarded.

A Manostat-Digipet, having a maximum delivery capacity of 0.1 ml. with divisions of 10^{-4} ml., forced organic liquid to be diffused by the water into the capillary tubing. The Digipet, organic feed reservoir, and capillary were connected through a three-way teflon stopcock. Connectors were ball-and-socket joints to the Digipet and feed reservoir with an O-ring seal to the capillary. Teflon O-rings were used to prevent any dissolution of sealing compound.

The organic drop suspended on the top of the capillary was magnified and projected on to a HIP 8 mm. movie projector scope. Magnification was approximately 23 times, with calibration carried out by using known volumes of nonsoluble liquid from the Digipet. As a further calibration check, glass beads of known diameter were also used. Light source was a Federal microfilm reader-projector equipped with a heat filter meniscus lens.

Organic liquid densities were determined by weighing in a pycnometer. Interfacial densities were determined by pycnometer using saturated solutions. Solubility was determined by preparing known volumes of organic in water, measuring the refractive index of the solutions, and determining the amount of organic in a saturated solution of organic and water by its refractive index. Refractive index was measured by using a Baush and Lomb optical refractometer, and viscosity by a Ostwald capillary viscometer.

Procedure

The reservoir was filled with distilled water and the immersion pump started to insure a constant volume of water in the constant head tank. At this point the valve to the rotameter with the desired flow range was opened to the full open position. The needle valve was then opened to bring water-flow rate to the desired value. Water flow was maintained for a few minutes to insure a steady flow rate. The Digipet was filled from the organic reservoir. The stopcock was then opened to the digipet, and a drop was formed on the tip of the capillary using the digipet, after which the stopcock was closed. This drop was always larger than the desired drop to nullify the first diffusive effects which could be unsteady state and to allow damping of the drop oscillations caused by drop formation. When the drop diameter reached the largest calibrated diameter, a stopwatch was started and water flow rate noted. When the drop was diffused to the smaller known diameter, the stopwatch was stopped and the water flow rate again noted. Flow rate and time for the drop to diffuse between the two known

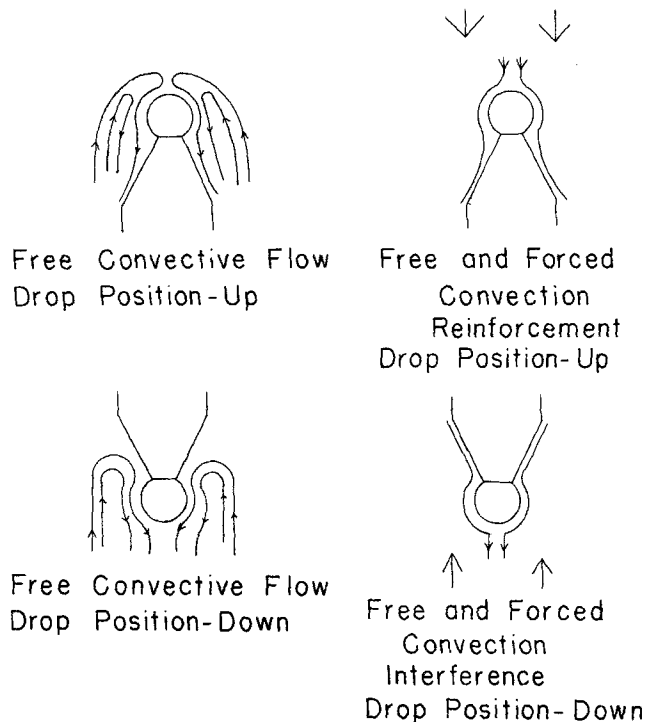


Fig. 3. Free and forced convection for interfacial density heavier than surrounding medium.

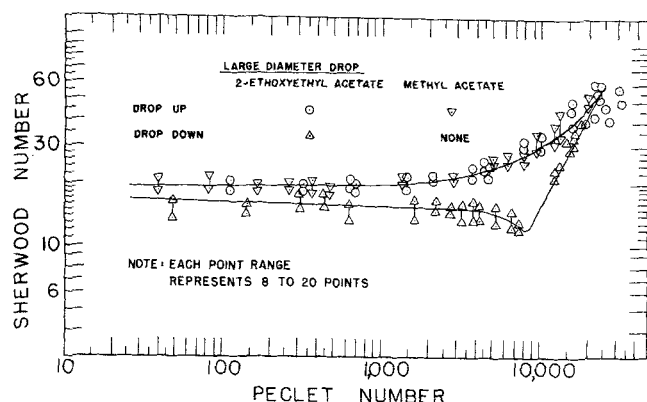


Fig. 4. Sherwood number vs. Peclet number, large drop.

diameters were tabulated.

Water temperature was measured in the discharge water, since at low flow rates water temperature approached room temperature. Calculations were then made for these individual temperatures.

DISCUSSION OF RESULTS

Experimental data were taken for liquid-liquid systems consisting of distilled water as the moving continuous phase and methyl acetate or 2-ethoxyethyl acetate as the organic liquid to be diffused. Data runs were made at flow rates selected to give a continuous curve of Peclet number from 0 to 35,000. At each flow rate, 8 to 20 runs were made, and data were plotted as a range of values of Sherwood number. Values of Sherwood number (and thus mass transfer rate) higher than predicted by diffusion theory in the Stokes flow region are attributed to free convective effects. This conclusion is reasonable as the density of the methyl acetate-water interface is greater than that of water in the bulk stream. Thus there are free convective mass-transfer effects which predominate at low ($N_{Pe} < 1,000$) or zero water flow rates giving higher transfer than that which would be predicted from diffusion alone. Also with the drop in the up position (Figure 3), water flow is in the same direction as the free convective currents, and thus reinforces rather than interferes with transfer. This effect has also been observed visually. Curves of Sherwood number vs. Peclet number (Figures 4 and 5) plotted from data taken with the drop in the down position (Figure 3) have a correspondingly lower value for Sherwood number for any given Peclet number. With the drop in the down position, free convective effect is opposed by the flow of water. This opposition reduces mass transfer rate by reducing the rate at which the organic flows away from the surface of the drop, and thus decreases concentration gradient at the organic-water in-

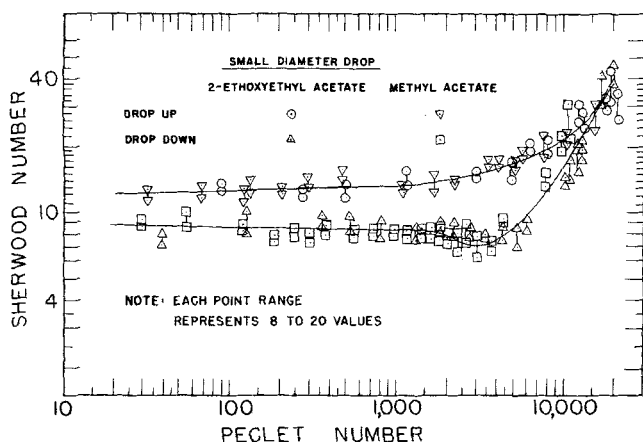


Fig. 5. Sherwood number vs. Peclet number, small drop.

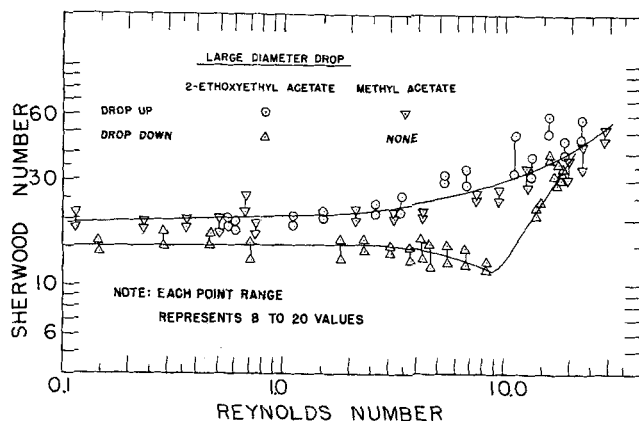


Fig. 6. Sherwood number vs. Reynolds number, large drop.

terface. As continuous phase flow is increased, opposition to free convection is increased until a reversal occurs in the effect which predominates. At this point a minimum of mass transfer occurs due to a reduced gradient, and thus a minimum Sherwood number occurs which corresponds to the valley in this curve. This minimum observed in the present work occurs at a Reynolds number between 6 and 9 (Figures 6 and 7) for Rayleigh numbers on the order of 10^4 to 10^5 and compares favorably with values of 20 to 60 observed by Garner and co-workers (6, 16, 21) for Rayleigh numbers on the order of 10^6 to 10^8 . With further increased flow rate, free convective effect is overcome, and mass transfer approaches transfer from the organic to the free stream rather than from the organic through a layer due to flow-opposed free convection and then to the free stream. Flow patterns indicative of the above have been visually observed in this apparatus.

To account for the differences in free convection, plots of Sherwood number divided by Rayleigh number to the one-fourth power vs. Peclet number have been prepared (Figures 8 and 9). These plots were made as to drop position (up or down). Figures 8 with the drop in the up position, has a divergence of $\pm 25\%$ from the median value at low Peclet number with convergence to a range of $\pm 12\%$ of the median value at high Peclet number (20,000). With the drop in the down position, slightly higher deviations are obtained. Figure 9 also indicates accounting for free convective effects by using $N_{Ra}^{1/4}$ does not change either the position as regards to flow or the decrease in Sherwood number resulting from free and forced convective effects interfering with each other.

Although a plot of N_{Sh} vs. N_{Ra} with N_{Pe} as a parameter would allow a value of the power on Rayleigh number to be more closely fitted to these particular data, the one-fourth power dependence on Rayleigh number was chosen because of its firm theoretical footing.

Examination of curves of $N_{Sh}/N_{Ra}^{1/4}$ vs. N_{Pe} (Figures

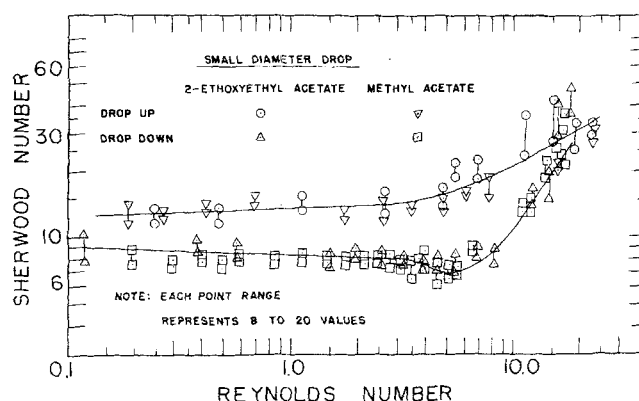


Fig. 7. Sherwood number vs. Reynolds number, small drop.

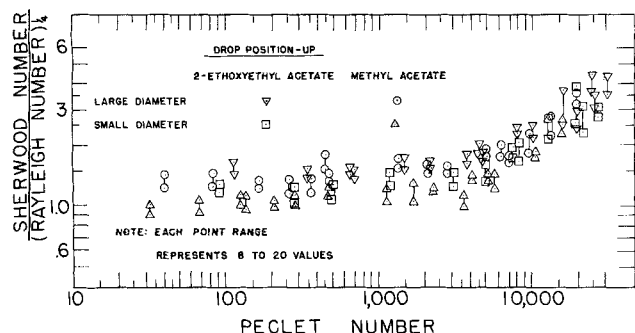


Fig. 8. Sherwood number over Rayleigh number to the one-fourth power vs. Peclet number, drop position: up.

8 and 9) shows a separation of the curves for the two drop positions until forced convection becomes predominant at high flow rates. This experimental evidence substantiates the concept of free convective mass transfer either interfering or reinforcing mass transfer at low flow rates. At zero flow rate, where diffusion and free convection alone influence the mass transfer rate, the curves originate from the same region. As flow rates increase, flow (and thus forced convection) reinforces free convective effect on the drop in the up position. With the drop in the down position, flow forces mass transferred by free convection back toward the drop, thus decreasing concentration gradient, driving force, and the amount of mass transferred. As the flow increases, free and forced convection reinforce each other with the drop in the up position, and interfere with each other with the drop in the down position (as has been discussed previously) until the flow becomes large enough to reverse the flow of mass transferred due to free convection.

The above statements, as regards enhancement and retardation of transfer with drop positions, apply to the case at hand where interfacial density is greater than that in the bulk. In situations where interfacial density is the lesser, the reverse of the above statements regarding enhancement and retardation is true.

The value for Sherwood number is considerably higher than that expected from forced convection alone and does not rapidly increase until flow rate has passed out of the Stokes flow region. Behavior such as this has been observed previously for much higher Rayleigh numbers (6) and was attributed to free convection. Data and experimental observations made in this study confirm these observations. Experimental data point to a mass transfer rate dependent in the low Reynolds number region upon free convective effects when density differences are present.

Curves obtained for the two organics are essentially the same with differences explained by inherent inaccuracy of the experimental system, and of physical property values. Graphs of Sherwood vs. Reynolds are also presented (Figure 6 and 7), but it should be noted that account has

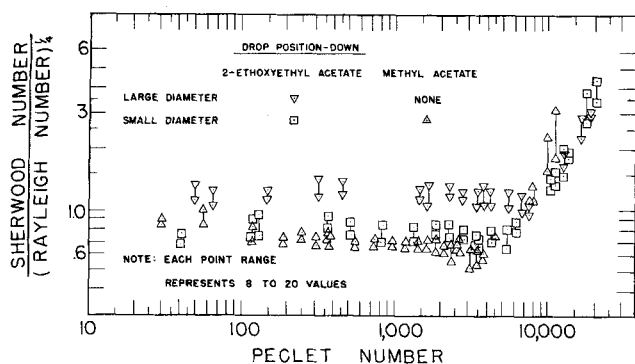
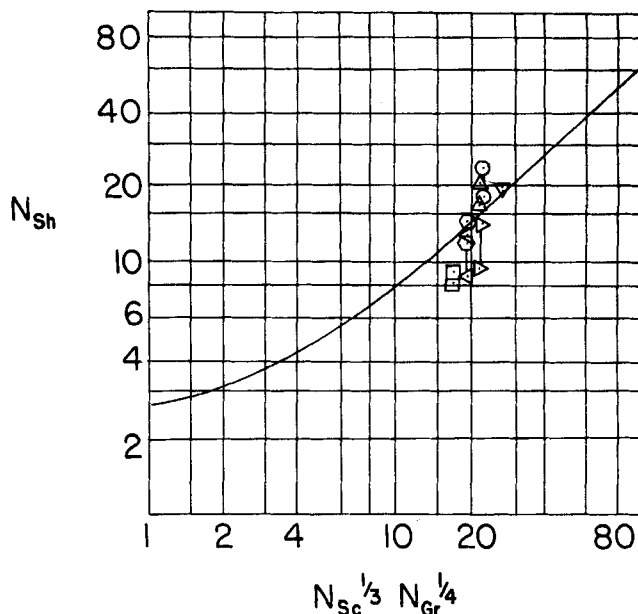


Fig. 9. Sherwood number over Rayleigh number to the one-fourth power vs. Peclet number, drop position: down.



	DROP	METHYL ACETATE	2-ETHOXYETHYL ACETATE
LARGE DIA.	UP	▽	○
	DOWN	NONE	△
SMALL DIA.	UP	▷	◁
	DOWN	◻	◉

NOTE: EACH POINT RANGE REPRESENTS 8 TO 20 VALUES

Fig. 10. Free convection from spheres, present data with Ranz-Marshall correlation.

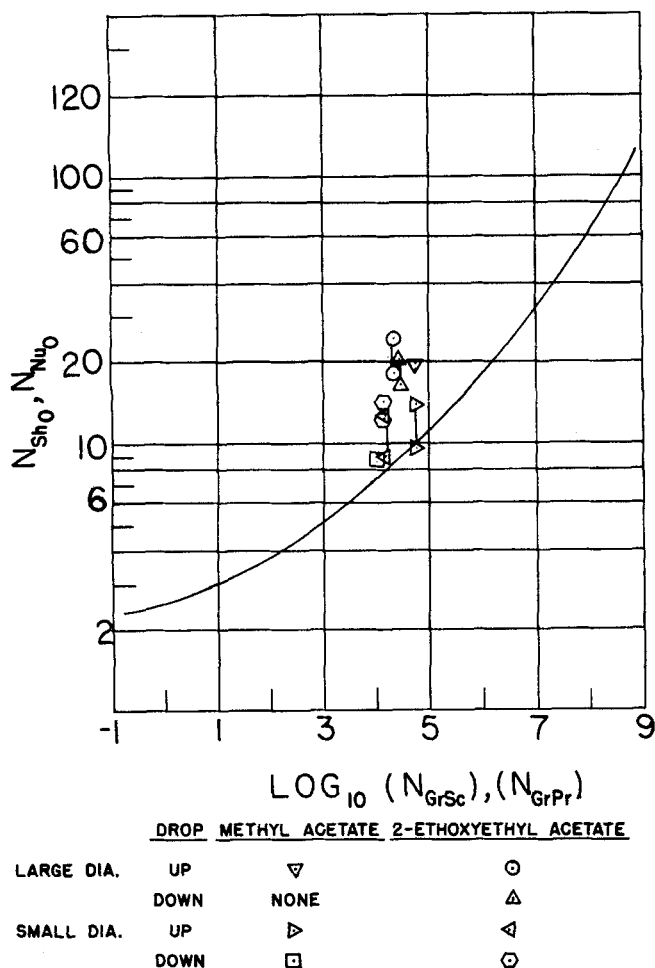
not been taken of Rayleigh and Schmidt number effects. Minimums in Sherwood number are noted for Reynolds numbers of approximately 6 and 9.

An attempt has been made to compare values, results, and possible correlations with the free convective work of other investigators. Ranz and Marshall (18) conducted experimental work in heat and mass transfer from drops. They developed a correlation and curve for free convection from spheres by using their data and free convective heat transfer data from other sources, as presented in Figure 10. Heat and mass transfer results are used interchangeably. Present results for both organics in the two drop diameters have been compared with this curve in Figure 10 with acceptable results.

Steinberger and Treybal (17) compared their equation for Sherwood number in free convection, their experimental data, and other free convection mass transfer data. Present results are incorporated with this comparison in Figure 11.

The experimental work and calculations involved in this study include a certain amount of error and inaccuracy. Diffusion coefficients were calculated by Wilke's correlation (19, 20) developed on the basis of the Stokes-Einstein equation. This equation is good for dilute solutions of nondissociating solutes to within $\pm 10\%$ of the actual diffusion coefficient.

Individual viscosities were determined experimentally by an Ostwald viscometer and a solution viscosity was then calculated. Densities were determined by pycnometer and are accurate to within 1%. Solubility of methyl acetate was obtained from the International Critical Tables. Methyl acetate used was 95% pure, with the remaining 5% methyl alcohol. The only 2-ethoxyethyl acetate available was "Practical" grade, which was distilled before using. A solubility curve was determined by refractive index. Accuracy of this determination is believed to be within 5%.



NOTE: EACH POINT RANGE REPRESENTS 8 TO 20 VALUES
Fig. 11. Free convection from spheres, present data with Steinberger and Treybal correlation.

Experimental values of time during data runs have varied as much as $\pm 8\%$. This is felt to be a combination of factors, prime of which is human error in deciding when a run started and ended. The drop as seen on the projector screen varied from a clear, well-defined circle for 2-ethoxyethyl acetate to clear oval surrounded by a dark shadow for methyl acetate (allowance was made for the shadow which appeared in the up position only). Drop diameter was reproducible and accurate to within approximately $\pm 5\%$ with much of this discrepancy again coming from human error. Care was exercised to start timing as the drop image passed the first predetermined diameter mark and to stop as it passed the second. A maximum error of ± 2 sec. is reasonable.

Most of the previous studies made in this manner involved dissolving a solid sphere into a liquid. This method loses sphericity of the test sphere, whereas the liquid drop was always spherical. Also constant surveillance is possible, and so free convective effects and film on the sphere become readily apparent. The positive physical factors of using a liquid are offset by (a) the larger angle subtended by the support system, (b) the fact that too great a density difference between sphere and water limits the size of the sphere, (c) the sphere has a tendency to dislodge from the support at high flow rates, and (d) the liquid sphere is vulnerable to physical factors such as thermal expansion.

These limitations were found to be a limiting factor in the case of methyl acetate, as the large diameter drop would not adhere to the tip in the down position due to

density differences between the pure methyl acetate and the distilled water. Neither methyl acetate nor 2-ethoxyethyl acetate would adhere to the tip at high flow rates, and this limitation appears to be the deciding factor in future liquid-liquid mass-transfer systems employing a liquid sphere.

CONCLUSIONS

Free convection at low flow rates (Reynolds number < 10 , Peclet number $< 1,000$) has significant reinforcing or retarding influence on mass transfer. If free convection interferes with mass transfer, Sherwood number will be less than in the case of enhancement, as has been shown in this work and by Garner and co-workers (6, 21) for higher Rayleigh numbers, until the flow rate is of sufficient magnitude to overcome the interfering effects of free convection. Previous correlations do not properly account for this effect, and so at low flow rates may be inaccurate, depending upon the relative enhancement or retardation effect of free convection.

Up to this time there has been little investigation centered around the effect of free convection at low flow rates ($Pe < 1,000$). Garner and co-workers' investigations, at higher Rayleigh numbers, produced mass transfer depressions for spheres in both the up and down position. Experimental evidence presented in this study shows mass transfer to be depressed in the case of free convective interference only; in the case of reinforcement, mass transfer will be raised continually. Experimental results are satisfactorily correlated in this study as $N_{Sh}/N_{Ra}^{1/4}$ vs. N_{Pe} .

ACKNOWLEDGMENT

The authors wish to thank the Colorado School of Mines Foundation, Inc. for financial support of this project.

NOTATION

- A = area of cross section of pyrex flow tube, sq.cm.
- C_p = specific heat, cal./g. °C.
- D_{AB} = diffusion coefficient, sq.cm./sec.
- D_{LM} = log mean diameter of drop, cm.
- g = gravitational acceleration, g.-cm./g.-sq.sec.
- N_{Gr} = Grashof number, modified for mass transfer, $\frac{\rho g D_{LM}^3 \Delta \rho / (\mu_{int})^2}{\mu_{int}}$
- h = heat transfer coefficient, cal./sq.cm. sec. °C.
- k = thermal conductivity, cal./cm. sec. °C.
- N_{Nu} = Nusselt number, $h D_{LM}/k$
- N_{Pe} = Peclet number, $D_{LM} V_{MAX}/D_{AB}$
- N_{Pr} = Prandtl number, $C_p \mu_{int}/k$
- N_{Ra} = Rayleigh number, $N_{GrSc} = \frac{g D_{LM}^3 \Delta \rho / \mu_{int}}{D_{AB}}$
- N_{Re} = Reynolds number, $\frac{D_{LM} \rho_{int} V_{MAX}}{A \mu_{int}}$
- N_{Sc} = Schmidt number, $\mu_{int}/\rho_{int} D_{AB}$
- N_{Sh} = Sherwood number, $\frac{\Delta V \rho_{pure}}{\pi D_{LM} \rho_{AO} D_{AB} t}$
- N_{Sho} = value of N_{Sh} at $N_{Re} = N_{Pe} = 0$
- t = time for drop to diffuse, sec.
- V_{MAX} = 2x volumetric fluid flow of system, cc./sec.
- ΔV = volume of organic drop diffused, cc.

Greek Letters

- $\Delta \rho$ = density difference between interfacial density and water density, g./cc.
- μ = shear viscosity of organic, g./cm.-sec.
- μ_{int} = interfacial viscosity, g./cm.-sec.
- μ_w = shear viscosity of water, g./cm.-sec.
- ρ_{pure} = density of pure organic, g./cc.
- $\bar{\rho}$ = average density of interfacial density and water density, g./cc.
- ρ_{AO} = density of organic interface, g./cc.
- ρ_{int} = interfacial density, g./cc.

LITERATURE CITED

1. Vliet, G. C., and G. Leppert, *J. Heat Transfer*, 163 (May, 1961).
2. Yuge, T., *ibid.*, 82, 214 (1960).
3. Kramers, H., *Physica*, 12, 61 (1946).
4. Briggs, D., W. Brown, M. Larson, P. McCuen, and J. Mitchell, Mech. Eng. 232 Lab., Stanford Univ., (1958), unpublished.
5. Williams, G. C., D.Sc. thesis, Mass. Inst. Tech., Cambridge, Mass., (1942).
6. Garner, F. H., and R. B. Keey, *Chem. Eng. Sci.*, 6, 119 (1958).
7. Steele, L. R., and C. J. Geankoplis, *AIChE J.*, 5, 178 (1959).
8. El-Wakil, M. M., G. E. Myers, and R. J. Schilling, *J. Heat Transfer*, 399 (Nov., 1966).
9. Ranz, W. E., and W. R. Marshall, Jr., *Chem. Eng. Prog.*, 48, 141 (1952).
10. Friedlander, S. K., *AIChE J.*, 3, 43 (1957).
11. *Ibid.*, 7, 347 (1961).
12. Yuge, T., *Rept. Inst. High Speed Mechanics*, Tohoku Univ., 57, 148, (1956).
13. Griffith, R. M., *Chem. Eng. Sci.*, 12, 198 (1960).
14. Acrivos, Andreas, *AIChE J.*, 4, 285 (1958).
15. Szewczyk, A. A., *J. Heat Transfer*, 501 (Nov., 1964).
16. Garner, F. H., and R. B. Keey, *Chem. Eng. Sci.*, 9, 218 (1958).
17. Steinberger, R. L., and R. E. Treybal, *AIChE J.*, 6, 227 (1960).
18. Ranz, W. E., and W. H. Marshall, Jr., *Chem. Eng. Progr.*, 48, 173 (1952).
19. Bird, R. B., W. E. Stewart, and E. N. Lightfoot, "Transport Phenomena," p. 515, John Wiley, New York (1964).
20. Sherwood, T. K., and R. C. Reid, "The Properties of Gases and Liquids," p. 51, McGraw-Hill, Pennsylvania, (1958).
21. Garner, F. H., and J. M. Hoffman, *AIChE J.*, 6, 579 (1960).

Manuscript received October 9, 1967; revision received January 9, 1968; paper accepted January 13, 1968.

Iterative Techniques in Optimization

I. Dynamic Programming and Quasilinearization

E. STANLEY LEE

Kansas State University, Manhattan, Kansas

The quasilinearization technique is used to overcome the dimensionality difficulties of dynamic programming. The approach is based on the fact that if the difference or differential equations are linear, their closed forms of solution can be obtained. This solution permits us to separate the effects due to the initial state from the effects due to the control variables. By using this separation combined with quasilinearization, the dimensionality of the functional equation of dynamic programming can be reduced to one in most cases. First, the optimization problem in cross-current extraction with discontinuous objection function is used to illustrate the technique. Then the technique is generalized to systems of difference and differential equations with fairly general objective functions.

Multistage optimization techniques can be divided into two general classes. The first class of techniques are the classical methods which include the calculus of variations and both the continuous and the discrete versions of the maximum principle. Various difficulties are encountered in solving optimization problems numerically by the classical methods. In the first place, considerable computational difficulties exist for the solution of the optimization problem if the number of the state variables are large. For continuous optimization problems these difficulties are known as the boundary-value difficulties, since they are caused by the numerical solution of large dimensional two-point boundary-value problems. A second difficulty in applying the classical methods arises from the inequality constraints which involve the state variables only. Inequality constraints involving the control variables, or involving both the control and the state variables, are fairly easy to handle numerically (1). However, this is not the case for inequality constraints involving the state variables only. Control variable is, in a sense, an independent variable and is not subject to differential or algebraic equation constraints. State variables are not independent. A trial and error or iterative procedure is generally used to treat inequality constraints on state variables. The third difficulty concerns the problem of true optimum. Both the calculus of variations and the maximum principle do not guarantee a true optimum. In fact, the Euler-Lagrange equations only give a stationary point. Whether this stationary point is a maximum, minimum, or just a saddle point, it must be

determined from physical or other considerations. A fourth difficulty is the inability of the classical method to handle nonanalytic objective functions easily.

The second class of optimization technique is the dynamic programming technique. This technique can handle state variable inequality constraints. It also can obtain the true optimum if proper search techniques are used. Furthermore, it is most suited for treating problems with non-analytic objective functions. However, severe difficulties exist when the number of state variables is moderately large. These difficulties are known as the dimensionality difficulties which are caused principally by the limited rapid-access memory of current computers. Although the dynamic programming technique does not have the other three difficulties, the dimensionality difficulties limit this technique to the optimization of problems with two, or to the maximum, three state variables.

Although various iterative techniques such as the functional gradient technique (2 to 4), the second variational method (5, 6), and the quasilinearization technique (1, 7) have been devised to overcome the boundary-value difficulties, little work has been done in using these iterative techniques to overcome the dimensionality difficulties in dynamic programming. In this paper, the quasilinearization technique, or the Newton-Raphson method for discrete systems, will be used to overcome these dimensionality difficulties. A set of recurrence relations are first obtained by the quasilinearization technique from the origi-